Different regimes of nucleation of superconductivity in mesoscopic superconductor/ferromagnet hybrids

N. Schildermans,[1] A. Yu. Aladyshkin,[2] A. V. Silhanek,[1] J. Van de Vondel,[1] and V. V. Moshchalkov[1]

[1]*Institute for Nanoscale Physics and Chemistry (INPAC), Nanoscale Superconductivity and Magnetism & Pulsed Fields Group,*
K.U. Leuven, Celestijnenlaan 200D, B-3001 Leuven, Belgium

[2]*Institute for Physics of Microstructures, Russian Academy of Sciences, GSP-105, 603950 Nizhny Novgorod, Russia*

The competition between two regimes of the nucleation of superconductivity is investigated experimentally and theoretically in a mesoscopic disk-shaped superconductor/ferromagnet hybrid. By changing the magnetic state of a multilayered Co/Pt disk one can reversibly affect the magnetic-field dependence of the critical temperature $T_c(H)$ of an Al layer. We demonstrate that an enhancement of the magnetic field near the edge of the out-of-plane magnetized disk either stimulates the nucleation of superconductivity at the disk perimeter due to the field compensation effect or prevents it due to edge magnetic barrier (for relatively low $|H|$ values). As a consequence, the presence of such magnetic-field pattern makes it possible to eliminate boundary effects for mesoscopic superconducting samples. Switching from one nucleation regime to another while sweeping H leads to an abrupt change of the slope of the $T_c(H)$ envelope.

　　　　PACS number(s): 74.78.Na, 74.25.Dw, 74.78.Fk

The coexistence of superconductivity and magnetic order has been intensively studied for several decades (see review[1] and references therein). Recent achievements in nanotechnology make it possible to prepare hybrid superconductor/ferromagnet (S/F) structures and study experimentally different aspects of the nontrivial interaction between the S and F components. In the case of spatially separated S and F subsystems, when the direct exchange of electrons at the interface between the two materials becomes suppressed, the interaction is dominated by the slow decaying magnetic fields $\mathbf{b}(\mathbf{r})$ induced by the ferromagnet. In particular, the inhomogeneous $\mathbf{b}(\mathbf{r})$ field generated by magnetic domains in the F layer affects strongly the nucleation of the superconductivity in the S layer and leads to exotic dependences of the critical temperature T_c on an external magnetic field H.[2–9] Indeed, the presence of inhomogeneous fields results in the appearance of places where the transverse component of the total magnetic field $|b_z(\mathbf{r})+H|$ reaches a local minimum and thus the nucleation of localized superconductivity in thin superconducting films will be promoted due to the field compensation effect.

The sample's imperfections or boundaries also stimulate the appearance of localized superconductivity in real samples.[10] As a result, a competition between different regimes of the order-parameter (OP) nucleation leads to additional modifications of the phase boundary $T_c(H)$. The OP nucleation in S/F hybrids with different competing confinements was recently studied theoretically in Refs. 3–6, 8, and 9. For example, for a generic S/F hybrid, consisting of a mesoscopic superconducting disk and a small magnetic particle, theory predicts two well-defined regimes: superconductivity can nucleate either near the disk center (under the magnetic particle) or at the disk edge. Switching between these regimes induced by varying the external field has been predicted to result in an abrupt change of the slope of $T_c(H)$.[5] These important theoretical findings have not yet been verified experimentally.

In this work we check experimentally the theoretical predictions for the superconducting OP nucleation in mesos-copic S/F hybrids consisting of S and F disks of the same diameters. We clearly demonstrate that the enhancement of the magnetic field near the disk perimeter is able to act as a magnetic potential barrier for the superconducting condensate. Interestingly, an effective suppression of the edge OP nucleation makes it possible to eliminate boundary effects inherent for all mesoscopic superconducting samples.[3,11] In addition, we show that the onset of the most favorable nucleation regime manifests itself as a clear change in the slope of $T_c(H)$.

The sample under investigation is a 50 nm thick Al disk with a diameter of 1.7 μm, covered by a ferromagnetic [0.4 nm Co/1.0 nm Pt]$_{10}$ multilayer, with a well-defined out-of-plane magnetization.[7] The S and F layers are separated by a 5 nm thick insulating Si layer in order to exclude the exchange interaction. Since the lateral size of the ferromagnetic disk is rather large, the as-grown and demagnetized states of such ferromagnet consist of multiple bubble domains. After applying an external field H_m of the order of the coercive field of the ferromagnet ($H_c \simeq 1$ kOe at $T=5$ K), it is possible to obtain nonzero remanent magnetization close to saturation. The higher the H_m value, the larger the averaged residual magnetization $\langle M_z \rangle$ of the sample.[7]

We have carried out measurements of the electrical resistance R as a function of temperature T and external field H in a four-probe geometry injecting a bias current through symmetrically attached leads (see Fig. 1). In order to investigate the influence of the magnetic domains on the nucleation of superconductivity the measurements were done using the same sample but for different magnetic histories (in particular, $H_m=2.0$, 2.5, and 3.4 kOe). During resistance measurements the maximal H field was always kept much lower than H_c, allowing us to assume that the residual distribution of magnetization has not been considerably changed. Using the measured dependencies $R(H,T)$, we reconstructed the phase boundary $T_c(H)$ based on the criterion $R(H,T_c)=0.1~R_n$, where R_n is the normal-state resistance.

Figure 2 summarizes the evolution of the $T_c(H)$ line for different remanent states of the sample. For a comparison the
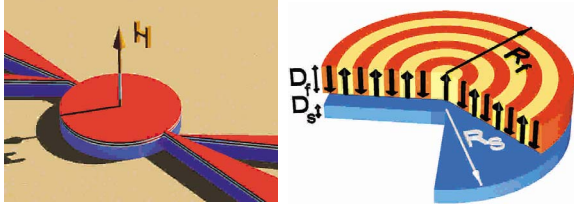
FIG. 1. (Color online) Left panel: schematic presentation of experimental system under consideration, where the bottom (blue) layer represents the S film, while the top one is the F layer. Symmetrically attached current/voltage leads were used for the transport measurements. Right panel: schematic presentation of the S/F sample used for modeling: R_s (R_f) and D_s (D_f) are the radius and the thickness of the S (F) disk. The magnetized states of the F layer are approximated as single-domain states, while for the demagnetized states a multidomain concentric ring structure is introduced.

$T_c(H)$ of a coevaporated reference Al disk (without magnetic layer on top) is also included. This phase boundary shows Little-Parks oscillations, indicating changes of vorticity in the system by one flux quantum.[3,12] The hybrid sample in the demagnetized state (curve $H_m=0$ in Fig. 2) shows a strong suppression of T_c as compared with the reference sample. A slightly asymmetric boundary in this case depends on the magnetic history and possibly reflects imperfections of the degaussing procedure resulting in a certain imbalance between positive and negative domains. After magnetizing the S/F hybrid in a positive external field H_m, a clear displacement of the T_c maximum toward negative H values is observed. In addition to this displacement, for the magnetized states the $T_c(H)$ lines become highly asymmetrical with respect to the position of the T_c maximum. Indeed, for stronger negative fields (at the left side of the T_c maximum) the average slope $s=|dT_c/dH|$ and the Little-Parks oscillations reproduce the phase boundary of the Al disk, whereas for weak negative fields (to the right of the T_c maximum) the slope s becomes steeper and Little-Parks oscillations are less pronounced and dependent on $\langle M_z \rangle$.

In order to explain the observed modification of the phase boundary of the mesoscopic S/F hybrid, we considered the
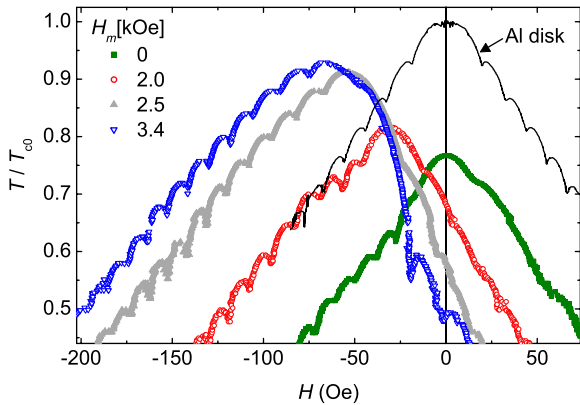

FIG. 2. (Color online) The phase-transition lines $T_c(H)$ obtained experimentally according to a 0.1 R_n criterion for four different magnetic states of the same S/F sample. The black solid curve corresponds to the $T_c(H)$ of an Al reference disk.

OP nucleation in a superconducting disk of radius R_s and finite thickness D_s, placed at a distance h below the ferromagnetic disk of the same radius and thickness D_f in the framework of the Ginzburg-Landau (GL) theory (for more details of the model see Ref. 5). The key issue in the modeling is the proper choice of the distribution of the out-of-plane magnetization M_z. In order to describe an effect of the magnetic domains inside the ferromagnet on $T_c(H)$, we consider a concentric magnetic structure (see Fig. 1). All domain walls are assumed to be cylinders of radius $r_{dw}^{(i)}$ and the local magnetization equals the saturated magnetization M_s (or $-M_s$) for positive (negative) domains. Even though this assumption represents a simplifications of the real magnetic pattern, it allows us to take into account the magnetic confinement typical for S/F hybrids with bubble domains.[8,9]

The vector potential induced by a uniformly magnetized disk, $M_z(r)=M_s$, can be calculated as follows:[4]

$$a_\theta^{(1)}(r,z) = 4M_s \sqrt{\frac{R_f}{r}} \int_{D_s+h}^{D_f+D_s+h} \frac{dz'}{k} \left[\left(1 - \frac{k^2}{2}\right)K - E \right],$$

where $k^2 = 4rR_f/[(r+R_f)^2+(z-z')^2]$, $K(k)$ and $E(k)$ are the complete elliptic integrals,[13,14] and (r, θ, z) is the cylindrical reference system. Thus, the uniformly magnetized disk with an aspect ratio $R_f/D_f \gg 1$ creates a highly inhomogeneous distribution of the magnetic field characterized by two length scales D_f and R_f: (i) the z component of the field reaches a maximal value $B_{max} \simeq \pi \langle M_z \rangle$ (for $h \ll D_f$) in a ringlike region of the width of the order of D_f near the disk edge and (ii) the field in the central part of the F disk varies quite slowly in space and a typical amplitude can be estimated as $B_0 \simeq 2\pi \langle M_z \rangle D_f/R_f \ll B_{max}$.

Provided that the widths of the domain walls are much smaller than other length scales, the magnetic field induced by a single circular domain is similar to that generated by a current loop of radius $r_{dw}^{(i)}$ (see Ref. 13). Summing up the fields induced by each domain, one can get an additional component,

$$a_\theta^{(2)}(r,z) = 8M_s \sum_{i=1}^{N_{dw}} (-1)^i \sqrt{\frac{r_{dw}^{(i)}}{r}} \int_{D_s+h}^{D_f+D_s+h} \frac{1}{k_i}$$
$$\times \left[\left(1 - \frac{k_i^2}{2}\right)K(k_i) - E(k_i) \right] dz',$$

where $k_i^2 = 4rr_{dw}^{(i)}/[(r+r_{dw}^{(i)})^2+(z-z')^2]$ and N_{dw} is the number of the domain walls.

Let us choose the total gauge in the form $A_{r,z}=0$ and $A_\theta(r,z) = a_\theta^{(1)}(r,z) + a_\theta^{(2)}(r,z) + Hr/2$, where H is the external magnetic field oriented along the z axis. Then due to the cylindrical symmetry the angular momentum L of the Cooper pairs (vorticity) is conserved,[5,6] and the solution of the linearized GL equation can be generally found in the form of the giant vortex $\Psi(\mathbf{r}) = f(r,z)e^{iL\theta}$. The $f(r,z)$ function should be determined from the following two-dimensional boundary problem:

$$-\frac{\partial^2 f}{\partial r^2} - \frac{1}{r}\frac{\partial f}{\partial r} - \frac{\partial^2 f}{\partial z^2} + \left(\frac{2\pi}{\Phi_0}A_\theta - \frac{L}{r}\right)^2 f = \frac{f}{\xi^2},$$
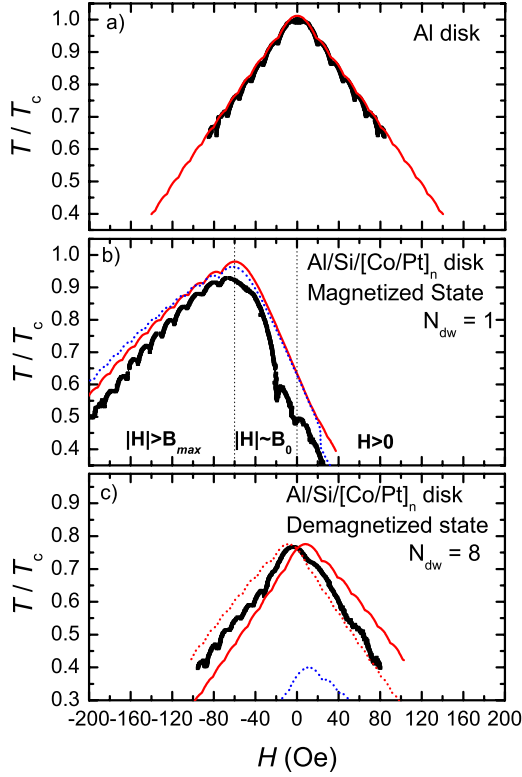
FIG. 3. (Color online) Experimental $T_c(H)$ curve (symbols) together with the theoretical fit (a) for the Al reference disk using the fitting parameters: $M_s=0$, $T_{c0}=1.275$ K, and $R_s=0.825$ μm. (b) For the magnetized S/F hybrid using the same parameters and for $M_s=325$ Oe, $D_s \rightarrow 0$ (blue dashed curve) and $D_s=50$ nm (red solid curve). (c) For the demagnetized S/F hybrid using $N_{dw}=8$, $M_s=325$ Oe, $D_s \rightarrow 0$ (blue dashed curve), and $D_s=50$ nm [red solid (dashed) curve, corresponds to the domain configuration with the last magnetic domain positive (negative)].

$$\left.\frac{\partial f}{\partial z}\right|_{z=0,D_s} = 0, \qquad \left.\frac{\partial f}{\partial r}\right|_{r=R_s} = 0. \qquad (1)$$

Here $\xi=\xi_0(1-T/T_{c0})^{-1/2}$ is the superconducting coherence length, T_{c0} is the critical temperature at $H=0$, and $\Phi_0 = \pi\hbar c/e$ is the flux quantum. As usual, the minimal eigen-

value $(1/\xi^2)_{\min}$ of Eq. (1) determines the critical temperature $T_c=T_{c0}[1-\xi_0^2(1/\xi^2)_{\min}]$.

The calculated $T_c(H)$ dependencies are compared with the experimental data in Fig. 3. The $T_c(H)$ for a plain S disk is shown in panel (a) and is very similar to the experimental curve using the following fitting parameters: $R_s=0.825$ μm, $M_s=0$, $T_{c0}=1.275$ K, and $\xi_0=160$ nm.

The phase boundary for the magnetized S/F system is compared with calculations in panel (b) of Fig. 3. The mentioned shift of the main T_c maximum can be explained by field compensation in the disk center. Indeed, applying a weak negative external field (i.e., $|H| \simeq B_0$) results in a vanishing of the total magnetic field in a broad central part of the superconducting disk. At the same time, the enhancement of the b_z component near the disk edge acts as magnetic barrier for the superconducting condensate and prevents the edge nucleation of superconductivity even in small-sized superconductors [see panel (b) of Fig. 4]. As a result, near this compensation field superconductivity nucleates first in the center of the superconducting disk in the form of a vortex-free state ($L=0$). Since the surface superconductivity becomes effectively suppressed, the OP nucleation in the mesoscopic S/F sample in this field range should be somehow similar to that typical for bulk superconducting samples and the reduced critical temperature T_c/T_{c0} will be close to $1-|H|/H_{c2}^0$, with H_{c2}^0 the upper critical field at $T=0$.[10]

In contrast, for rather high negative fields ($|H| \gg B_0$) due to the compensation effect a minimal value of the total magnetic field reaches at the edge of the disk [panel (a) of Fig. 4], and the edge OP nucleation will be promoted. Therefore, in this field range the oscillatory phase boundary is shifted toward negative H for fields of the order of $B_{\max}$. In addition, the slope s becomes close to T_{c0}/H_{c3}^0, typical for mesoscopic superconductors, with $H_{c3}^0 \simeq 1.69H_{c2}^0$ the critical field of surface superconductivity at $T=0$.[10] Thus, the observed change in the slope of the phase boundary can be attributed unambiguously to modifications of the conditions for the OP nucleation, caused by a competition between surface nucleation and magnetic confinement of the superconducting condensate.

A second change of the $T_c(H)$ slope, corresponding to the restoration of the edge nucleation regime, is expected at positive H values. Since the ratio between the total magnetic
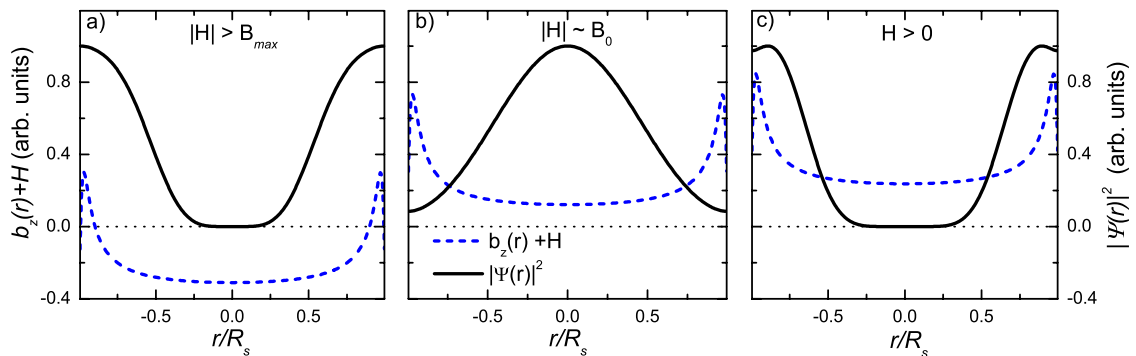

FIG. 4. (Color online) The examples of the spatial distribution of the total magnetic field $B_z=b_z(x)+H$ as well as the OP profiles $|\Psi(x)|^2$ calculated at the top surface of the superconducting disk ($z=D_s$) (a) for a strong negative field, $|H|>B_{\max}$, (b) for a weak negative field $|H|\sim B_0$, and (c) for a positive field $H>0$.

field at the edge $H+B_{max}$ and in the center $H+B_0$ goes to unity for increasing H value [panel (c) of Fig. 4], the magnetic barrier no longer prevents the edge OP nucleation. Corresponding with this second change of slope, a huge change in vorticity is expected from $L=0$ to $L=5$. The experimentally observed strong dip in T_c at $H \simeq -20$ Oe can be attributed to an entrance of a giant vortex. The discrepancy between the theoretically predicted transition field (at $H \simeq 13$ Oe) and the experimentally observed position can be ascribed to the approximate character of the model which ignores imperfections of the sample boundaries and nonaxial symmetry of the stray magnetic field, both tending to reduce the magnetic barrier at the sample border. We emphasize that a partly suppressed surface superconductivity for $H>0$ makes the conditions for the OP nucleation near the sample edge less favorable than at negative H values, resulting in less pronounced Little-Parks oscillations in the positive field region.

The calculated phase boundary for the demagnetized S/F sample is shown in panel (c) of Fig. 3. Here we assume the presence of circular bubble domains inside the ferromagnet with domain walls equally distributed along the r axis. According to magnetostatics, the narrower the magnetic domains, the more inhomogeneous the field over the sample

thickness will be.[8] Therefore, in order to obtain the strong general suppression of T_c and a reasonable phase boundary, one should take into account both the field and OP variations in the z direction.

In conclusion, we have demonstrated experimentally and theoretically that the conditions for the nucleation of superconductivity in a mesoscopic S/F hybrid can be strongly modified by the magnetic confinement produced by a ferromagnetic layer. A field-induced transition from the OP nucleation in the center of the structure toward its boundaries can be clearly identified as a pronounced asymmetry in the phase boundary and an abrupt change of the slope of the envelope of the $T_c(H)$ dependence.

[1] J. Flouquet and A. Buzdin, Phys. World **15** (1), 41 (2002); I. F. Lyuksyutov and V. L. Pokrovsky, Adv. Phys. **54**, 67 (2004); A. I. Buzdin, Rev. Mod. Phys. **77**, 935 (2005).

[2] Y. Otani, B. Pannetier, J. P. Nozières, and D. Givord, J. Magn. Magn. Mater. **126**, 622 (1993); A. Yu. Aladyshkin, A. I. Buzdin, A. A. Fraerman, A. S. Mel'nikov, D. A. Ryzhov, and A. V. Sokolov, Phys. Rev. B **68**, 184508 (2003); M. Lange, M. J. Van Bael, Y. Bruynseraede, and V. V. Moshchalkov, Phys. Rev. Lett. **90**, 197006 (2003); Z. Yang, M. Lange, A. Volodin, R. Szymczak, and V. V. Moshchalkov, Nat. Mater. **3**, 793 (2004); W. Gillijns, A. Yu. Aladyshkin, M. Lange, M. J. Van Bael, and V. V. Moshchalkov, Phys. Rev. Lett. **95**, 227003 (2005); M. V. Milošević and F. M. Peeters, *ibid.* **94**, 227001 (2005).

[3] L. F. Chibotaru, A. Ceulemans, M. Morelle, G. Teniers, C. Carballeira, and V. V. Moshchalkov, J. Math. Phys. **46**, 095108 (2005).

[4] C. Carballeira, V. V. Moshchalkov, L. F. Chibotaru, and A. Ceulemans, Phys. Rev. Lett. **95**, 237003 (2005).

[5] A. Yu. Aladyshkin, D. A. Ryzhov, A. V. Samokhvalov, D. A. Savinov, A. S. Mel'nikov, and V. V. Moshchalkov, Phys. Rev. B **75**, 184519 (2007).

[6] A. Yu. Aladyshkin, A. S. Mel'nikov, and D. A. Ryzhov, J. Phys.: Condens. Matter **15**, 6591 (2003).

[7] W. Gillijns, A. V. Silhanek, and V. V. Moshchalkov, Phys. Rev. B

74, 220509(R) (2006).

[8] A. Yu. Aladyshkin and V. V. Moshchalkov, Phys. Rev. B **74**, 064503 (2006).

[9] W. Gillijns, A. Yu. Aladyshkin, A. V. Silhanek, and V. V. Moshchalkov, Phys. Rev. B **76**, 060503(R) (2007).

[10] See, e.g., M. Tinkham, *Introduction to Superconductivity* (McGraw-Hill, New York, 1996), Chap. 4.

[11] H. J. Fink and A. G. Presson, Phys. Rev. **151**, 219 (1966); V. V. Moshchalkov, L. Gielen, C. Strunk, R. Jonckheere, X. Qiu, C. Van Haesendonck, and Y. Bruynseraede, Nature (London) **373**, 319 (1995); A. K. Geim, I. V. Grigorieva, S. V. Dubonos, J. G. S. Lok, J. C. Maan, A. E. Filippov, and F. M. Peeters, *ibid.* **390**, 259 (1997); V. A. Schweigert and F. M. Peeters, Phys. Rev. B **57**, 13817 (1998); H. T. Jadallah, J. Rubinstein, and P. Sternberg, Phys. Rev. Lett. **82**, 2935 (1999); L. F. Chibotaru, A. Ceulemans, V. Bruyndoncx, and V. V. Moshchalkov, Nature (London) **408**, 833 (2000).

[12] W. A. Little and R. D. Parks, Phys. Rev. Lett. **9**, 9 (1962).

[13] L. D. Landau and E. M. Lifshitz, *Electrodynamics of Continuum Media*, 2nd ed. (Pergamon, Oxford, 1984).

[14] *Handbook of Mathematical Functions*, Natl. Bur. Stand. Appl. Math. Ser. No. 55, edited by M. Abramowitz and I. A. Stegun (U.S. GPO, Washington, DC, 1965).